

Physics 134L: Photometric Redshift Survey

Physics Department, University of California, Santa Barbara

Santa Barbara, CA 93106, USA

(Dated: June 13, 2023)

Abstract

In this experiment, two methods were used to compute the photometric redshift, z_{phot} , of six galaxies. One method utilized the public domain code hyperz, while the other utilized nearest neighbor machine learning. Of the six galaxies, images and data of four were obtained using the LCO telescope system, while the other two were obtained from the SIMBAD astronomical database for testing the methods. One galaxy, 2dFGRS TGN132Z253, had data from both SIMBAD and from experimental data. For the six galaxies, the percent differences from the accepted redshift for each using hyperz were 12900%, 353%, 801%, 274%, 42.5%, 6038%, and 18500%. The percent differences using the nearest neighbor method were 9430%, 439%, 781%, 174%, 10.6%, 43.2% and 85.9%. These results show that while the results of computing photometric redshift using the telescope available yields inaccurate results, it is likely that a more powerful telescope that would yield more accurate results and make finding photometric redshift a useful way to compute many redshifts quickly.

I. INTRODUCTION

A. Redshift

Redshift is a phenomena that results from the fact that the universe is expanding. Since most of the objects in the universe are moving away from us, the observed wavelength of an object usually appears longer than it actually is due to the Doppler effect. The speed at which objects move away from us is dependent on their distance from us, meaning that redshift is also dependent on distance. The redshift of an object is

$$z = \frac{\lambda_{obs} - \lambda_{em}}{\lambda_{em}} = \frac{H_0}{c}r \quad (1)$$

where λ_{obs} is the observed wavelength, λ_{em} is the emitted, unshifted wavelength, H_0 is the Hubble constant, c is the speed of light, and r is the distance between Earth and the object.[1]

Studying redshift is important because it can tell us information about how fast the universe is expanding and can be used to determine how far away distant objects are.

One way that redshift can be found is using spectroscopy. Electrons in an atom can absorb photons of specific wavelengths in order to transition to a higher energy level. If light from an object passes through gasses such as the hydrogen, nitrogen, and helium produced in a star's atmosphere, then the photons of specific wavelengths will be absorbed, creating an absorption spectra. This absorption spectra can be viewed using a spectrograph and then the shift in absorption lines can be analyzed to figure out the redshift of that object.

However, the telescopes available to us do not have spectroscopic capabilities, so a different method of determining redshift needs to be used. Photometric redshifts can be determined by analyzing the magnitudes of an object in different filters and comparing the

differences. In this experiment, we used photometry to estimate redshifts of galaxies, as will be further explained later. [2]

B. Magnitude

The magnitude at wavelength λ_0 is traditionally defined as

$$m_{\lambda_0} = -2.5 \log \left(\frac{e(\lambda_0)}{e_0} \right) = -2.5 \log e(\lambda_0) + q_0 \quad (2)$$

where $e(\lambda)$ is the monochromatic flux from the star and e_0 is the flux from a reference object and is absorbed into the constant, q_0 , which defines an object of magnitude zero. This system of measuring magnitude is usually calibrated around the Vega star and so is called the Vega magnitude system.[2]

The amount of light flux a telescope can take in is dependent on the sensitivity function of its filter, $t_0(\lambda)$. This means that the apparent magnitude of a star through a filter is given by

$$m_{\lambda_0} = -2.5 \log \int_0^\infty t_0(\lambda) e(\lambda) d\lambda + 2.5 \log \int_0^\infty t_0(\lambda) d\lambda + q_{\lambda_0} \quad (3)$$

Using different filters on a telescope determines what wavelengths of light will be captured from the object. The transmission functions for the SDSS filters used in this experiment by the Las Cumbres Observatory (LCO) telescopes are shown in Figure 1.[3]

Something to note when using SDSS filters is that it was noticed that when objects were viewed through SDSS from different locations, there were differences between expected and measured magnitudes.[4] To adjust for this error and ensure that the magnitudes of fainter objects are, a new magnitude system was created for when data is taken using SDSS filters. This system is called the asinh magnitude system and defines magnitude as

$$m = -\frac{2.5}{\ln(10)} \left[\operatorname{asinh} \left(\frac{(f/f_0)}{(2b)} \right) + \ln(b) \right] \quad (4)$$

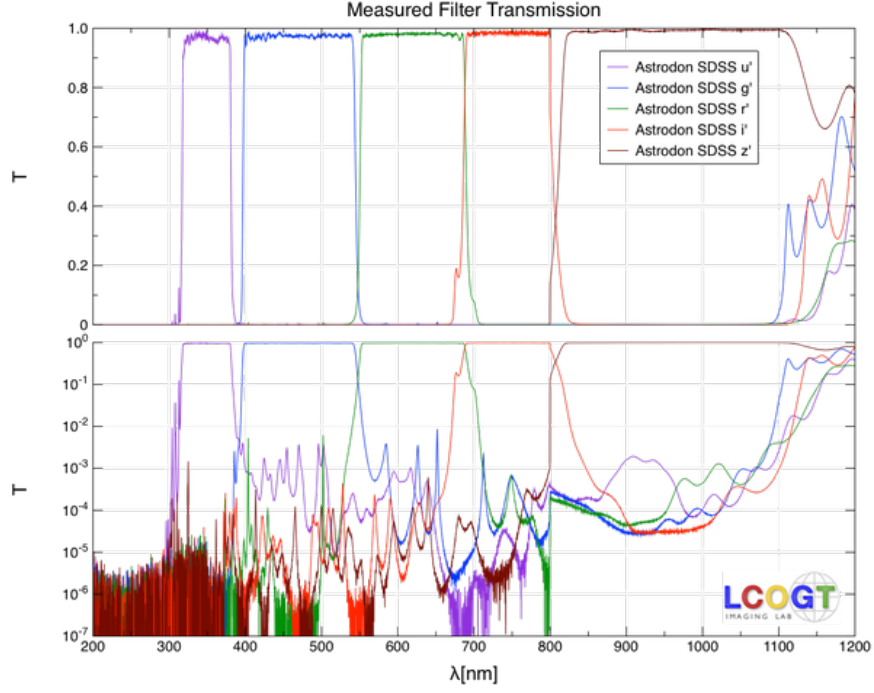


FIG. 1: The transmission functions for the SDSS u'g'r'i'z' filters.[3].

where f is the flux of an object, f_0 is the flux of a 0 magnitude object seen through the filter, and b is the softening parameter.[5] The softening parameter depends on the filter and its values are shown in Table I.

Band	b	Zero-Flux Magnitude $[m(f/f_0 = 0)]$
u	1.4×10^{-10}	24.63
g	0.9×10^{-10}	25.11
r	1.2×10^{-10}	24.80
i	1.8×10^{-10}	24.36
z	7.4×10^{-10}	22.83

TABLE I: The softening parameter and zero-flux magnitude for each filter band.[4]

Understanding magnitudes is important in this experiment because the differences of the magnitudes in an object in different filters, known as color indices, can be used to determine photometric redshift. Two methods of determining photometric redshift from magnitudes are used in this experiment, hyperz and nearest neighbor, and they are discussed in the following section.

II. METHODS

A. Las Cumbres Observatory Data Collection

Images were taken from LCO using LCO's 0.4m SBIG Telescope and the SDSS g' , r' , and i' filters. It was originally decided to use the SDSS u' , g' , r' , and i' filters because those four filters would cover the visible spectrum with no gaps, which is needed to perform photometry. However, it was determined that the u' filter was not useful in this experiment because the magnitudes and fluxes of objects were not able to be distinguished from noise in the image. An example of an image taken in the r' filter compared to the u' filter can be seen in Figure 2.



FIG. 2: An example demonstrating why data was not able to be taken taken in the u' filter (right) compared to other filters like the r' filter (left).

The galaxies we took images of were chosen with the recommendation from Professor Lubin and our TA Jeongwha Kim about how the telescopes could not detect objects with a magnitude greater than approximately 16. More distant objects will have a greater magnitude (be dimmer) and so we wanted to choose galaxies that had the highest redshifts possible that could still be detected by LCO’s telescopes. We used the 6dF Galaxy Survey (6dFGS) to find galaxies that had magnitudes around 16 which also gave us their expected redshifts.[6]

In order to get good visualization of the magnitude 16 objects, an exposure time t of 100 s was chosen along with multiple exposures for each galaxy so that more accurate data could be taken. The exposure time determines how long the aperture of the telescope is open and so an exposure time needed to be chosen that is long enough for the galaxy to be seen but not so long as to be overexposed. The exposure time was determined using test images to ensure that these requirements were fulfilled. The number of exposures determines how many times an image is taken of the same object using the same filter and exposure time, so more exposures allows averaging of data that will diminish the effect of outliers and ensure more accurate results.

An additional galaxy, the Sombrero Galaxy (NGC 4594) was also chosen because it was pretty and would provide a good example of the difference in magnitudes between different filters. The chosen targets, along with their coordinates (given as Right Ascension and Declination under the 2000 epoch) and details about their exposures are shown in Table II.

B. BANZAI

Images taken by LCO telescopes undergo a cleaning process referred to as the BANZAI (“Beautiful Algorithms to Normalize Zillions of Astronomical Images”) pipeline. All data

Galaxy Name	RA (hh:mm:ss.ss)	Dec(hh:mm:ss.ss)	SDSS Filters	N	t (s)
NGC 4594 (Sombrero Galaxy)	+12 : 39 : 59.43	−11 : 37 : 22.97	u',g',r',i'	5	100
g1227523-112037	+12 : 27 : 52.30	−11 : 20 : 37.1	g',r',i'	10	100
g1246208-424138	+12 : 46 : 20.79	−42 : 41 : 38.0	g',r',i'	10	100
g1258223-030606	+12 : 58 : 22.25	−03 : 06 : 05.7	g',r',i'	10	100

TABLE II: The coordinates where the telescope was aimed towards for each galaxy and which filters were used to capture the galaxy, along with the number of exposures per filter, N , and exposure time t . The first galaxy is the only one not taken from the 6dFGS.[6]

used in this experiment were processed through the BANZAI program. This program includes bad-pixel masking which compensates for dead pixels and other systematic errors in the telescope using sigma clipping, which masks any pixels that deviate too much from the median flux value. It also helps to reduce noise through bias subtraction. Noise is caused by imperfect transfer between sensor and computer or imperfect image capture, and bias subtraction is taking a bias image, usually when the telescope is covered, and subtracting it from the final image. Dark subtraction is also used to reduce the effect of heat generated over long exposures causing the image to have light spots. Dark subtraction is subtracting a long exposure image taken from the original image. BANZAI processing also performs flat field correction which corrects flaws in the image caused by how the curvature of the lens creates a darkening effect around the image's edges. LCO takes bias, dark, and flat field images every day of various exposure times to ensure accurate images after BANZAI processing.[7]

The BANZAI pipeline also does source extraction. SEP is the "Python and C library for Source Extraction and Photometry" and performs many functions, the most important

of which is source extraction.[8] Source extraction is finding stars and galaxies in an image and noting their coordinates, as well as finding the fluxes of these objects using different apertures. The aperture used in this experiment to find flux was the Kron aperture, and will be described in more detail in a later section. The BANZAI pipeline processes image information using SEP and produces a FITS file with SEP information such as object coordinates and fluxes. The right ascension and declination coordinates are calibrated using astrometry.net.[9]

An example of an image before and after BANZAI processing can be seen in Figure 3

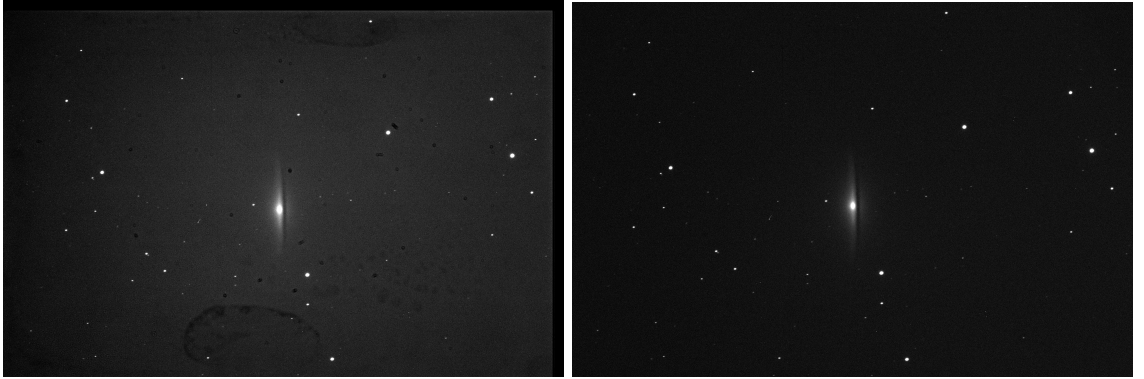


FIG. 3: An example of an image before (left) and after (right) BANZAI processing.

The data used in this experiment can be found in [this Google Drive folder](#).

C. Determining Magnitudes

Both the hyperz and nearest neighbors methods take in magnitudes as an input to determine photometric redshift. To determine the magnitudes of objects in the telescope image, the flux from several Kron apertures determined by the BANZAI pipeline was used. Kron’s algorithm allowed the flux of a star to be estimated within rings of a certain radius, r_{kron} . [10]

In a circular aperture, ϵ , this is given by,

$$r_{kron} = \frac{\sum_{i \in \epsilon} r_i p_i^{(d)}}{\sum_{i \in \epsilon} p_i^{(d)}} \quad (5)$$

where $p_i^{(d)}$ is the pixel value in the detection image at pixel i (the image centered around the source but not the entire image) and r_i is the distance from the centroid of the source.[11]

90% of the flux of an object is captured inside a circle of radius $2r_{kron}$. The total flux is then given by the sum of the pixel values, $p_i^{(d)}$, inside the kron ellipse of radius $2r_{kron}$. [10]

To calculate magnitudes, the flux must be in units Joules/second. The fluxes from multiple exposures were averaged in each filter to get more accurate results. To get average flux values in Joules/second, F_f , use

$$F_f = \frac{\sum_i K_i \times G_i}{\sum_i t_i} \times (1.602 \cdot 10^{-19} J) \quad (6)$$

where f be the index for the filter type (g',r',i') i is the index for each fit file with filter f , K_i is the Kron peak flux in counts, G_i is the gain (electrons per count), and t_i is the exposure time.

Then, we used this summed flux, the reference fluxes from [5], and b values from Table I to find the asinh magnitudes of each our sources using Equation 4. To use this equation, the flux density from 6 must be found in units of janskys, which is done by dividing the flux by the area of the telescope and the bandwidth of each filter. The bandwidth is determined by finding the frequency of the central wavelength of each filter from Figure 1. f_0 is found to be 3631 jansky for each filter used in this experiment. The flux density value is in units of janskies, where there are $10^{-26} W * m^{-2} Hz^{-1}$ per jansky. The asinh magnitude error is calculated by the following equation:

$$m_{error} = \frac{2.5}{\ln(10)} \frac{err}{t \cdot 2b} \left(\frac{f}{f_0}\right) \sqrt{1 + \frac{(f/f_0)^2}{2b}}^{-1} \quad (7)$$

where *err* is the count error.

Both methods take magnitudes using the AB magnitude scale as inputs, which is defined by

$$m_{AB} = -2.5 \log\left(\frac{f_{AB}}{3631 Jy}\right) \quad (8)$$

where f_{AB} is the flux density in janskys.

One thing to note is that the SDSS asinh magnitudes are meant to be on the same scale as the AB system, but are slightly off in the u and z band filters.[12] However, since the telescope does not have a z filter and the u' filter was ignored, it was concluded that the experimental asinh magnitudes were equal to their equivalent AB magnitudes.[13]

D. Hyperz

One of the methods used to determine photometric redshift from the magnitudes of an object was hyperz. Hyperz is a coding package that takes a photometric catalog and then finds the photometric redshift of each object using Spectral Energy Distribution (SED) fitting.

To use hyperz, the user inputs a photometric catalog of objects that specifies their observed magnitudes (AB magnitudes were used) and corresponding errors. The program then transforms the magnitudes and errors into fluxes with the option of applying a dereddening for the galactic extinction to the photometric catalog. Since reddening is most important in the high-z universe and all of the objects observed in this experiment were low redshift, no dereddening was specified.

The program also simultaneously builds a hypercube consisting of the fluxes determined from template SEDs provided by hyperz and specified by the user. The template SEDs were

chosen to reproduce colors of galaxies of different spectral types. To do this, different models of Star Formation Rate (SFR) were used. One model of SFT uses Schmidt’s law which assumes that the rate of star formation varies with a power n of the density of interstellar gas. Assuming $n = 1$ and a closed-box model (constant total mass) leads to the analytic exponential approximation seen in Equation 9 where τ is the timescale. The standard five SEDs used in this program had SFRs of a single burst and exponential with timescale 1 Gyr (representing early galaxies), exponentials with timescale 3 Gyr and 15 Gyr (representing spiral galaxies), and constant SFR (representing irregular galaxies).

$$\psi(t) \propto e^{-t/\tau} \quad (9)$$

While building the hypercube, the spectra would be first reddened following one of five possible laws specified by the user (none were used as reddening is most relevant for high- z universe). Then, the spectra were depressed with the Lyman forest, which is formed because the spectra of high redshift galaxies suffer a drop in flux from absorbing neutral hydrogen clouds at different redshifts between the source and the observer. This also does not have much relevance for low redshift objects. To finish the hypercube, the spectra were convolved with user-provided filter response functions to obtain expected fluxes. These filter response functions can be seen above in Figure 1.

After the hypercube construction, the program does a chi-squared calculation that can be seen in Equation 10.

$$\chi^2(z) = \sum_{i=1}^{N_{Filters}} \left[\frac{F_{obs,i} - b \times F_{Temp,i}(z)}{\sigma_i} \right]^2 \quad (10)$$

$F_{obs,i}$ is the flux from the observed SED, $F_{Temp,i}$ is the flux from the template, σ_i is their uncertainty in filter i , and b is a normalization constant.[14] The program finds the best photometric redshifts solutions and probabilities by minimizing the chi-squared results. A

summary of the process used by the hyperz code can be seen in Figure 4.

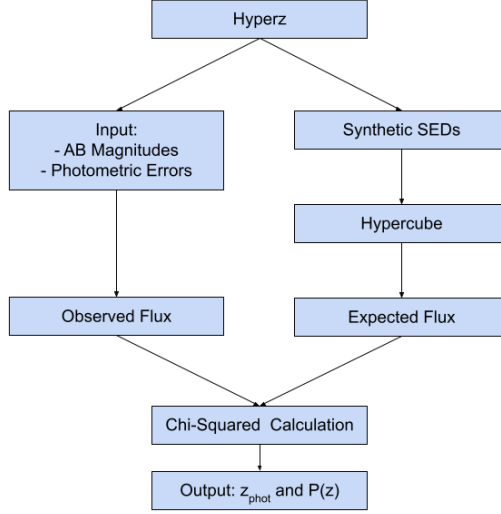


FIG. 4: This diagram summarizes the basic process of how hyperz takes an input photometric catalog and uses SED fitting to produce a photometric redshift estimate and probability.

E. Nearest Neighbors

The nearest neighbors method uses the k-Nearest Neighbor Algorithm and around 177,300 different celestial objects from the SDSS DR 17 database [15]. The code estimates a data point value based on the known k amount of neighbors of similar values. Let i be an index for our experimental galaxies in the query set and let j be an index for objects in the training set. Our nearest neighbors code attempts to minimize the following equation:

$$z_{phot} = c_i + a_i d_i \quad (11)$$

where z is the estimated photometric redshift, c is an offset term, d_i is a parameter vector value, and a is the coefficient vector for d . To do this, the concept of modeling a celestial object's nearest neighbors[?] using linear regression[16] is used. Our experiment utilizes 3 parameter values: r magnitude, $g-r$ color index, and $r-i$ color index. Color indices are the difference between the magnitude of an object found in two different filters.

The nearest neighbors to the inputted galaxies are determined by minimizing the chi-squared equation[?]:

$$\chi^2(z) = \sum_{j \in NN} \frac{(z_j - c_i - a_i d_j)^2}{w_j} \quad (12)$$

However, due to the difficult minimization method, our experiment utilizes a personal and more simple distance metric seen in Equation 13.

$$D = \sum_{j \in NN} |d_i - d_j| = \sum_{j \in NN} (r_i + g - r_i + r - i_i) - (r_j + g - r_j + r - i_j) \quad (13)$$

The distance metric D describes how different the training data is from the query data. The code calculates the distance metric between the inquiry galaxy and all objects in the training set. We set $k = 100$. This means the 100 objects with the smallest distance metric will be used to compute the predicted redshift value. Let NN be an index for all k objects that have the smallest distance metric. The predicted redshift is calculated as the average of all known redshifts in k :

$$z_{predicted} = \sqrt{\frac{\sum_{j \in NN} z_j}{k}} \quad (14)$$

And the error is given by:

$$\delta z_{phot,i} \approx \sqrt{\frac{\sum_{j \in NN} (z_j - z_{predicted})^2}{k}} \quad (15)$$

A flowchart summarizing how the nearest neighbors method works can be seen in Figure 5.

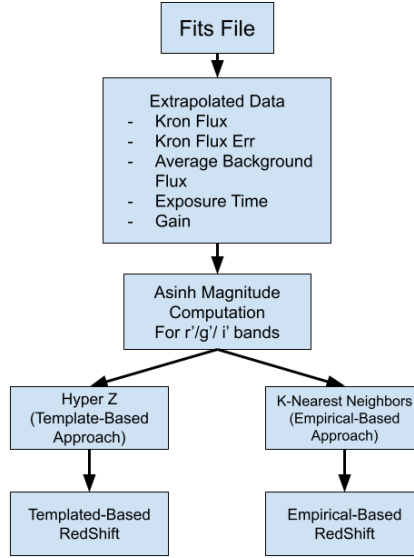


FIG. 5: This diagram summarizes the basic process of extrapolating data from the fits files and its conversion to photometric redshift using both the hyperz and nearest neighbors methods.

III. RESULTS

One result that may be of interest is how the fact that objects have different magnitudes in each filter can be used in many different ways. Not only can the different magnitudes be used to find photometric redshift, they can also be used to create pretty, colorful pictures. An example of how the trichromy method in AstroArt utilizes the different magnitudes in each filter to produce a pretty picture can be seen of the Sombrero Galaxy in Figure 6.

The main purpose of this experiment was still to use the different magnitudes in each filter to determine photometric redshift. After analyzing all of the images taken by the LCO telescope, it was realized that only one of our target galaxies was bright enough to give



FIG. 6: This is an example of a pretty picture that can be obtained using the fact that objects have different magnitudes in each filter.

flux results after being processed by the BANZAI pipeline. Because of this, other galaxies were found using the SIMBAD Astronomical Database that had coordinates and flux values provided in the fits files.[17] The galaxies used can be seen in Table III.

The magnitudes for each galaxy in each filter can be seen in Table IV. The galaxy letters denoted by *exp* are the galaxies where experimental magnitudes were found and the galaxy letters denoted by *acc* are accepted values found from the SIMBAD database.[17] One galaxy, *D*, had both experimental and accepted values for comparison.

The photometric redshift results from the hyperz method are given in Table V. The hyperz method did not return an error in redshift. Instead, it returned a chi-squared probability

Galaxy Letter	Galaxy Name	Accepted Redshift
A	NGC 4594 (Sombrero Galaxy)	0.003416 ± 0.000017
B	2MASX J12275231-1120370	0.08504 ± 0.00015
C	6dFGS gJ124555.9-424016	0.04768 ± 0.00015
D	2dFGRS TGN132Z253	0.11333 ± 0.00003
E	M101 (Pinwheel Galaxy)	0.000811 ± 0.000016
F	NGC 4151	0.003262 ± 0.000067

TABLE III: This table shows the galaxies with their accepted values of redshift, as well as their designated letters for ease of reference. Images of galaxies A-D were obtained using the LCO telescope system and galaxies E and F were taken from SIMBAD ([17]) for testing purposes.

	r' magnitude	r' error	g' magnitude	g' error	i' magnitude	i' error
A_{exp}	13.47746163	75.87	14.79941838	53.91	13.56564163	58.78
B_{exp}	20.5571003	2.68	21.70406992	2.22	20.96777631	2.41
C_{exp}	20.41815517	2.56	22.09272542	1.59	20.55157546	2.51
D_{exp}	19.38510287	3.44	20.70239522	3.02	19.61346501	3.05
D_{acc}	17.511	0.007	18.441	0.01	17.051	0.007
E_{acc}	11.529	0.002	12.219	0.002	11.237	0.002
F_{acc}	11.613	0.006	12.284	0.006	11.081	0.007

TABLE IV: This table shows the asinh magnitudes used to find photometric redshift. A_{exp} - D_{exp} were found using the experimental technique outlined above and D_{acc} - F_{acc} are accepted magnitude values from SIMBAD.[17]

that the result was correct, which is written in the table.

Galaxy	Accepted Redshift	Hyperz Redshift	Probability (%)	Percent Error
A_{exp}	0.00342 ± 0.00002	0.443	100.00	12900%
B_{exp}	0.0850 ± 0.0002	0.385	99.40	353%
C_{exp}	0.0477 ± 0.0002	0.430	99.33	801%
D_{exp}	0.113 ± 0.00003	0.423	99.81	274%
D_{acc}	0.113 ± 0.00003	0.065	97.63	42.5%
E_{acc}	0.000811 ± 0.000016	0.066	97.58	8038%
F_{acc}	0.00326 ± 0.00007	0.607	96.53	18500%

TABLE V: This table shows the redshifts obtained using the hyperz method. No errors in photometric redshift were given by the hyperz method and so the chi-squared probability is given instead.

Hyperz does not provide a specific error for the photometric redshift results and instead outputs a probability percentage that the predicted redshift value is correct. However, something noted in the hyperz manual is that when only three filters the results are not very reliable and there may be multiple solutions with high probability.[14] Additionally, the hyperz templates and program were meant to be used to calculate large redshifts and the lowest redshift value it can return is 0.05. Therefore, at low redshift values like the ones in our experiment, it is not expected to be very precise. This can be seen in the fact that most of hyperz results have a percent error over 100%. However, there were lower percent errors when using accepted values rather than experimental, indicating that while hyperz is not accurate for low redshifts, there was likely also significant error that came from magnitude calculations.

The photometric redshifts found using the nearest neighbors method can be seen in Table

VI.

Galaxy	Accepted Redshift	Nearest Neighbors Redshift	Percent Error
A_{exp}	0.00342 ± 0.00002	0.326 ± 0.449	9430%
B_{exp}	0.0850 ± 0.0002	0.458 ± 0.269	439%
C_{exp}	0.0477 ± 0.0002	0.420 ± 0.205	781%
D_{exp}	0.113 ± 0.00003	0.310 ± 0.105	174%
D_{acc}	0.113 ± 0.00003	0.125 ± 0.122	10.6%
E_{acc}	0.000811 ± 0.000016	0.000461 ± 0.000000	43.2%
F_{acc}	0.00326 ± 0.00007	0.000461 ± 0.000000	85.9%

TABLE VI: This table shows the redshifts obtained using the nearest neighbors method as compared to the accepted redshifts, as taken from SIMBAD.[17]

As compared to hyperz, the nearest neighbors method appeared to be more accurate. The error that was present was likely to at least partly come from statistical error from the training set. However, it was noticed that the percent error for galaxies using accepted values were all below 100%, demonstrating that a lot of error likely came from magnitude calculations. Additionally, the percent error appeared larger when the redshift of the galaxy got below 0.005, with the same results for both E_{acc} and F_{acc} . This indicates that the same 100 nearest neighbors were used for these galaxies, and they were the 100 galaxies with the lowest redshift. Even though there were 177,302 galaxies in the training set, only about 1,000 had redshifts below 0.1. Therefore, while the nearest neighbors method is more accurate, it also loses accuracy when the redshift of the object it is calculated is too low.

A plot of the photometric redshift results from both methods compared to the actual redshifts for each galaxy can be seen in Figure 7.

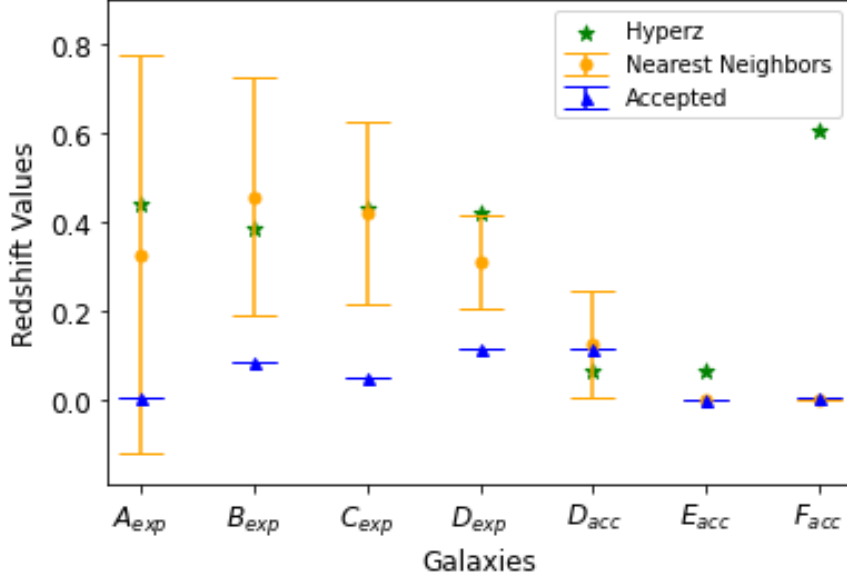


FIG. 7: This graph shows the redshift values obtained using the hyperz method, the Nearest Neighbors method, and the accepted values for each galaxy.

It is clear from both methods that there is significant error in how the magnitude was calculated. The systematic errors that could have contributed to this include: reddening, background flux, magnitude conversion, and quantum efficiency. While neither method took reddening into account, reddening is unlikely to have a large effect as all of the galaxies analyzed had low redshifts. Additionally, we did attempt to account for background flux by removing it before the magnitude calculation. Additionally, using the fact that the asinh and AB magnitude scales were equivalent in our magnitude conversion in the filters used was likely not a source of error as the significant differences are 0.02 and 0.04 magnitude difference in the u and z bands respectively.[12] However, slight differences for magnitudes in the g', r', and i' filters could be a source of systematic error. This can also come from the fact that the asinh magnitudes were designed for the SDSS u, g, r, i, z filters and not the g', r', and i' filters used.[4] Another possible source of error is quantum efficiency, which is a measure of the effectiveness of the detector. The quantum efficiency of the telescope

used was not taken into account in this experiment which could have caused a shift in the amount of flux detected by the telescope compared to the true flux value.

The data shows that using photometric redshift under the current astrophysical framework is not very accurate, especially with the equipment available to us. However, for high redshift galaxies that could be detected using more powerful telescopes, using these methods could be an effective way to quickly get many redshift results.

IV. DISCUSSION

Determining redshift is important for not only finding the rate at which the universe is expanding, but also to find out how far away distant objects in the universe are. For the second purpose, a photometric redshift survey can be extremely helpful because it can compute many results quickly and without requiring a telescope with a spectrometer. However, this is only true if a more powerful telescope is used that can detect objects at high redshifts. The telescope used in this experiment could barely detect objects with a magnitude around 16 and those galaxies had low redshifts less than 0.1.

If I had access to a better telescope, I would have targeted galaxies of much higher redshift and magnitude. Additionally, if the telescope was more able to detect objects in the u' filter, or had a z' filter, then more filters could have been used that would have increased the accuracy of both methods.

Overall, these results were not very accurate, likely due to incorrect magnitude conversions and only three filters being used. While they were more accurate when using accepted data, their accuracy still decreased when redshift became very low. However, if a more powerful telescope with more filters was used, with known magnitude conversions, then it is likely that both of these methods could produce accurate results and would be useful in

quickly computing many redshift values.

V. REFERENCES

- [1] Barbara Ryden. *Introduction to Cosmology*. Cambridge University Press, New York, NY, 2 edition, 2017.
- [2] Pierre Lena, Daniel Rouan, Francois Lebrun, Francois Mignard, and Didier Pelat. *Observational Astrophysics*. Springer, 3 edition, 2008.
- [3] Las Cumbres Observatory. Transmission functions. URL <https://lco.global/observatory/instruments/filters/>.
- [4] Chris Stoughton, Robert H. Lupton, Mariangela Bernardi, Michael R. Blanton, Scott Burles, et al. Sloan Digital Sky Survey: Early Data Release. *The Astronomical Journal*, 123(1):485–548, January 2002. doi: 10.1086/324741. URL <https://iopscience.iop.org/article/10.1086/324741/pdf>.
- [5] Robert H. Lupton, James E. Gunn, and Alexander S. Szalay. A Modified Magnitude System that Produces Well-Behaved Magnitudes, Colors, and Errors Even for Low Signal-to-Noise Ratio Measurements. *The Astronomical Journal*, 118(3):1406–1410, September 1999. doi: 10.1086/301004.
- [6] D. Heath Jones, Will Saunders, Matthew Colless, Mike A. Read, Quentin A. Parker, et al. The 6dF Galaxy Survey: samples, observational techniques and the first data release. *Monthly Notices of the Royal Astronomical Society*, 355(3):747–763, December 2004. doi: 10.1111/j.1365-2966.2004.08353.x.
- [7] Curtis McCully, Monica Turner, David Collom, and Matt Daily. *BANZAI Documentation, Release 0.23.0*, 5 2019.
- [8] Kyle Barbary. Sep: Source extractor as a library. *Journal of Open Source Software*, 1(6):58, 2016. doi: 10.21105/joss.00058. URL <https://doi.org/10.21105/joss.00058>.

- [9] Dustin Lang, David W. Hogg, Keir Mierle, Michael Blanton, and Sam Roweis. Astrometry.net: Blind astrometric calibration of arbitrary astronomical images. *The Astronomical Journal*, 139(5):1782–1800, March 2010. doi: 10.1088/0004-6256/139/5/1782.
- [10] R. G. Kron. *Photometry of a Complete Sample of Faint Galaxies*. PhD thesis, University of California, Berkeley, December 1978.
- [11] E. Bertin and S. Arnouts. SExtractor: Software for source extraction. *Astronomy and Astrophysics Supplement*, 117:393–404, June 1996. doi: 10.1051/aas:1996164.
- [12] J. B. Oke and J. E. Gunn. Secondary standard stars for absolute spectrophotometry. *The Astrophysical Journal*, 266:713, March 1983. doi: 10.1086/160817. URL <https://doi.org/10.1086/160817>.
- [13] R. C. Bohlin, M. E. Dickinson, and D. Calzetti. Spectrophotometric standards from the far-ultraviolet to the near-infrared: STIS and NICMOS fluxes. *The Astronomical Journal*, 122(4):2118–2128, October 2001. doi: 10.1086/323137. URL <https://doi.org/10.1086/323137>.
- [14] Micol Bolzonella, Joan-Marc Miralles, and Roser Pell’o. *HyperZ v1.2 User’s Manual*, 1999. URL http://www.bo.astro.it/~micol/Hyperz/hyperz_manual1.2.pdf.
- [15] Katherine Accetta, Conny Aerts, Victor Silva Aguirre, Romina Ahumada, Nikhil Ajgaonkar, N Filiz Ak, Shadab Alam, Carlos Allende Prieto, Andres Almeida, Friedrich Anders, et al. The seventeenth data release of the sloan digital sky surveys: Complete release of manga, mastar, and apogee-2 data. *The Astrophysical Journal Supplement Series*, 259(2):35, 2022.
- [16] Photometric redshifts for the SDSS Data Release 12. *Monthly Notices of the Royal Astronomical Society*, 460(2):1371–1381, April 2016. ISSN 0035-8711. doi: 10.1093/mnras/stw1009. URL <https://doi.org/10.1093/mnras/stw1009>.
- [17] M. Wenger, F. Ochsenbein, D. Egret, P. Dubois, F. Bonnarel, et al. The SIMBAD astronomical

database. The CDS reference database for astronomical objects. , 143:9–22, April 2000. doi:
10.1051/aas:2000332.